Weak Inter- and Intralayer Exchange Coupling between Copper(II) Dimers and a Triplet Density Effect in EPR of Tris(ethylenediamine)cobalt(III) Bis(μ-chloro)bis[trichlorocuprate(II)] Dichloride Dihydrate

W. Hilczer, J. Goslar, J. Tritt-Goc, and S. K. Hoffmann*

Institute of Molecular Physics, Polish Academy of Sciences, Smoluchowskiego 17, PL-60179 Poznañ, Poland

Received March 23, 1994[⊗]

Low-temperature EPR spectra of $Co(en)_3CuCl_5 \cdot H_2O$ single crystals were studied at X-band. The crystals contain layers of antiferromagnetically coupled $Cu_2Cl_8^{4-}$ dimers, with singlet−triplet splitting $2J_0 = -14.8$ cm^{-1}, separated by diamagnetic $Co(en)_3$ molecules. Superexchange coupling between dimers located in neighboring layers, determined from the merging effect of EPR lines from inequivalent sites, is $J_1 = 0.00712$ cm^{-1} at room temperature, decreases to 0.00325 cm^{-1} below 100 K, and then is temperature independent. Below 15 K the fine structure lines from $S = 1$ are resolved with the following zero-field splitting parameters: $D_z = -0.0200$ cm^{-1}, $D_y = 0.0147$ cm^{-1}, and $D_x = 0.0053$ cm^{-1}. The appearance of the structure is a result of a decrease in the number of magnetic dimers due to a rapid thermal depopulation of the triplet state when $kT < 2J_0$. A detailed analysis of this process allowed us to determine intralayer exchange coupling between dimers which amounts to $J_2 = 0.041$ cm^{-1} at 100 K and decreases on cooling following triplet density $\varrho(T) = [1 + {}^1/_3 \exp(-2J_0/kT)]^{-1}$ behavior. Hyperfine splitting is not resolved down to 4.2 K, and the relatively narrow lines indicate a strong mobility of the still remaining triplet excitons. The line width decreases on cooling down to about 100 K, and then a strong broadening appears resulting in the fine structure splitting. Contributions from the narrowing effect, triplet state density, and temperature variations of the zero-field splitting have been separated in $\Delta B_{pp}(T)$. A decrease in the zero-field splitting occurs on heating and, in the temperature range 4.2−100 K, is phenomenologically described by the equation $D(T) = D_0(1 - aT - bT^{-2})$.

Introduction

EPR is a powerful tool in studies of the local electronic and magnetic structure of paramagnetic centers. In paramagnetic crystals, however, the local properties are overdominated by interionic interactions which mask the individual properties of paramagnetic complexes, and EPR can be used as a method for studying interionic couplings. Information regarding the dipolar and exchange coupling is contained in experimental g-factors and line width ΔB_{pp} of the EPR spectrum which as a rule consists of a single resonance line.

How these couplings influence the g-factors of magnetically inequivalent sites in a crystal is very well recognized for copper(II) ions with $S = {}^1/_2$, and appropriate procedures to obtain molecular g-factors from experimental data have been proposed.[1−3] In contradiction to this, the line width angular and especially temperature dependencies are not satisfactorily described by any theory. Classical theories of magnetic resonance line shapes based on correlation function behavior[4] work adequately only when dipolar interaction produces a Gaussian distribution of the local magnetic field and, in addition, these fields are time-modulated in a random way by exchange interaction. A contribution from dynamically averaged hyperfine structure can be calculated by means of the hyperfine second-moment M_2^{hf} in the strong exchange limit.[5] Difficulties appear, however, when inequivalent Cu(II) sites exist in a crystal and when exchange coupling, dipolar coupling, hyperfine splitting, and splitting from inequivalent sites are comparable one to another, because they have different contributions at different crystal orientations and are differently affected by temperature. We have solved this problem, to some extent, presenting an algorithm for a "decoupling" of the EPR lines from inequivalent sites.[6,7] This algorithm allows one to calculate "true" EPR parameters, i.e. g-factors and ΔB_{pp}, and it simultaneously gives the exchange coupling integral between inequivalent sites.

In this paper we will show that the algorithm we initially used for a description of isotropic Heisenberg superexchange coupling effect between inequivalent sites can be successfully applied to an "effective" exchange coupling governed by thermal triplet state density $\varrho(T) = [1 + {}^1/_3 \exp(-2J_0/kT)]^{-1}$ in antiferromagnetic dimers as well as can describe an averaging of the zero-field splitting of the copper(II) dimeric units. Moreover we will subtract the effect of inequivalent sites, unresolved zero-field splitting, and thermal triplet density from experimental ΔB_{pp} data which allow us to determine values of two small interdimer exchange integrals operating between layers and within layers of $Co(en)_3CuCl_5 \cdot H_2O$ crystals.

The orthorhombic crystal structure of $Co(en)_3CuCl_5 \cdot H_2O$ is built of layers of $Cu_2Cl_8^{4-}$ parallel to the *ab* crystal plane, which are well separated by large diamagnetic Co(ethylenediamine)$_3^{3+}$ molecules.[8,9] The crystal unit cell contains four centrosymmetric dimers with a molecular structure presented in Figure 1. The

* To whom correspondence should be addressed. Phone: +48-61-612407. Fax: +48-61-684524. e-mail: skh@marta.ifmpan.poz.edu.pl.

⊗ Abstract published in *Advance ACS Abstracts*, March 1, 1995.

(1) Hathaway, B. J.; Billing, D. E. *Coord. Chem. Rev.* **1970**, *5*, 142.
(2) Hoffmann, S. K.; Szczepaniak, L. S. *J. Magn. Reson.* **1983**, *52*, 182.
(3) Hoffmann, S. K.; Goslar, J.; Szczepaniak, L. S. *Phys. Rev. B* **1988**, *37*, 7331.
(4) Kubo, R.; Tomita, K. *J. Phys. Soc. Jpn.* **1954**, *9*, 888.
(5) Borras-Almenar, J. J.; Coronado, E.; Gatteschi, D.; Gomez-Garcia, C. J.; Zanchini, C. *J. Phys. Chem.* **1993**, *97*, 4206.
(6) Hoffmann, S. K. *Chem. Phys. Lett.* **1983**, *98*, 329.
(7) Hilczer, W.; Hoffmann, S. K. *Chem. Phys. Lett.* **1988**, *144*, 199.
(8) Hodgson, D. J.; Hale, P. K.; Hatfield, W. E. *Inorg. Chem.* **1971**, *10*, 1061.

0020-1669/95/1334-1852$09.00/0

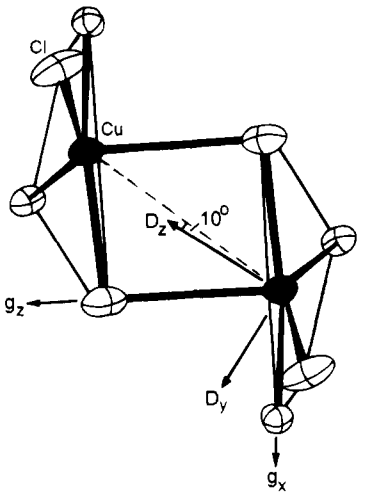

Figure 1. Molecular structure of the $[Cu_2Cl_8]^{4-}$ dimer in the $Co(en)_3CuCl_5 \cdot H_2O$ crystal.[8,9] The local axes of the **g**-tensor and the dimer zero-field splitting tensor are marked. The g_y and D_x axes are perpendicular to the dimer plane.

dimers are nearly identically oriented, i.e. magnetically equivalent, in the layers, with a local z axis of an individual $CuCl_5^{3-}$ complex (g_z-axis in Figure 1) lying close to the *bc*-plane and with an angle $2\gamma = 66°$ between the z-axes of neighboring layers. The copper(II) ions are relatively strongly antiferromagnetically coupled in dimeric species with singlet−triplet splitting $2J_0 = -14.8$ cm^{-1},[9,10] which is temperature independent. Our previous EPR studies[9] in the temperature range 77−370 K have shown that the zero-field splitting is not resolved and a very weak interlayer exchange coupling decreases linearly on cooling. EPR measurements at 4.2 K show that fine structure lines resulting from zero-field splitting are resolved as an effect of a depopulation of the magnetic triplet state.[10] In this paper we will present the detailed studies of the EPR behavior in the temperature range below 77 K where anomalous variations in line width are observed and where gradual separation of the fine structure lines appears.

Experimental Section

The compound $Co(en)_3CuCl_5 \cdot H_2O$ was prepared according to the method of ref 11. Single crystals were grown from a water solution as brown prisms with well-developed (001) plane.

EPR spectra were recorded on a Bruker ESP380E FT/CW operating at X-band (9.8 GHz) equipped with a dielectric TE_{011} resonator and 100 kHz magnetic modulation. A flowing helium Oxford CF935 cryostat was used to obtain temperatures above 4 K. The temperature was stabilized with an accuracy ±1 deg in the whole temperature range. The rotational data were collected in the *abc* crystal axis reference frame.

Results and Discussion

Angular Dependencies and EPR Parameters. EPR spectra of $Co(en)_3CuCl_5 \cdot H_2O$ crystal recorded at room temperature and at 4.2 K differ significantly. At room temperature the spectrum consists of two resonance lines from magnetically inequivalent dimers in neighboring layers which we discussed in the previous paper.[9] Angular dependencies of the resonance field and line width are shown in Figure 2. EPR shows that the dimers marked as I and II in one layer and dimers III and IV in a second layer are magnetically equivalent giving only two Lorentzian

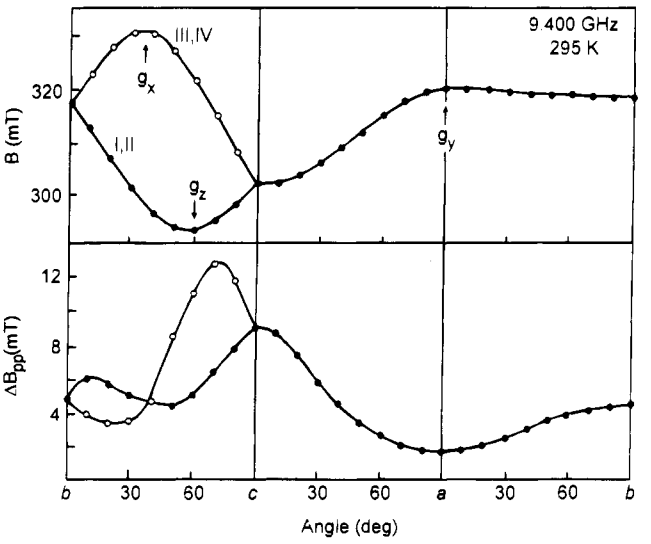

Figure 2. Angular dependence of the resonance field B and line width ΔB_{pp} at room temperature. Solid lines on $B(\theta)$ plots are the best fit to the tensor equation $g^2 = \alpha + \beta \cos 2\theta + \gamma \sin 2\theta$. I−IV mark the four dimers in the unit cell (see Figure 4). Solid lines on $\Delta B_{pp}(\theta)$ dependence are guides to the eyes only.

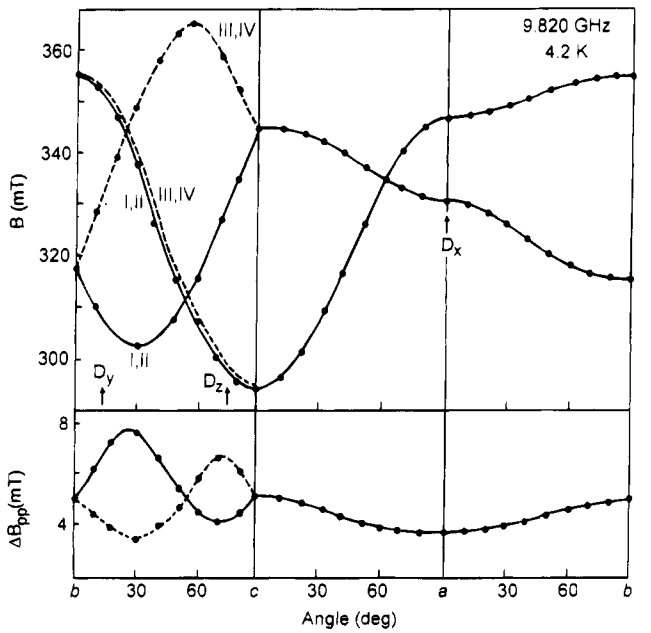

Figure 3. Fine structure (zero-field splitting) doublets and line width ΔB_{pp} angular dependence at 4.2 K for I−IV dimers. The lines on $B(\theta)$ dependence are theoretical plots with data of the Table 1. Positions of the x, y, and z axes of the **D** tensor are marked.

lines. At 4.2 K each of these two lines splits into a doublet characteristic for zero-field splitting of the triplet state $S = 1$. Angular behavior at 4.2 K is shown in Figure 3. So, the fine structure for copper(II) dimers with $S = 1$ is resolved at low temperatures but it is averaged out at high temperatures whereas the hyperfine splitting expected for Cu(II) is not resolved in the whole temperature range. The zero-field splitting at 4.2 K was analyzed by McGregor and Hatfield[10] although their experimental data were collected in a different laboratory system related to the crystal habit.

The g-tensor principal axes are determined by local crystal field symmetry at Cu(II) sites, and the g_z-axis is directed along the longer Cu−Cl arm of the dimeric bridge. The axes are shown in Figure 1 and marked on resonance field variations in Figure 2. The ground state of Cu(II) is $d_{x^2-y^2}$ in accordance with distorted square-pyramidal stereochemistry around Cu(II)

(9) Hoffmann, S. K.; Hodgson, D. J.; Hatfield, W. E. *Inorg. Chem.* **1985**, *24*, 1194.
(10) McGregor, K. T.; Hatfield, W. E. *J. Chem. Phys.* **1976**, *65*, 4155.
(11) McGregor, K. T.; Losee, D. B.; Hodgson, D. J.; Hatfield, W. E. *Inorg. Chem.* **1974**, *13*, 756.

Table 1. Spin Hamiltonian Parameters and Direction cosines at 4.2 K[a]

		direction cosines to the axis			
		a	*b*	*c*	ref 10
g_z	2.255	0	(+−−+) 0.5736	(+−+−) 0.8191	2.27
g_y	2.070	1	0	0	2.09
g_x	2.030	0	(−+−+) 0.8191	(+−−+) 0.5736	2.03
D_z	−200	0	(+−−+) 0.2588	(+−+−) 0.9652	195
D_y	147	0	(+−+−) 0.9652	(−++−) 0.2588	150
D_x	53	1	0	0	50

[a] *D*-values in 10^{-4} cm^{-1}. Errors: in *g*-factors, ±0.005; in *D*-values, ±4 cm^{-1}. Signs of the direction cosines of the dimers I−IV are given in parentheses: (I II III IV).

ion. The principal axis directions do not change appreciably when the temperature is lowered and when the zero-field splitting appears. It is confirmed by an analysis of the rotational data of Figure 3 using the spin-Hamiltonian

$$H = \mu_B \tilde{B}\cdot g\cdot S + \tilde{S}\cdot D\cdot S \quad (1)$$

For $g\mu_B B > D$ the allowed transitions in the triplet state can be written in the first-order approximation as

$$h\nu = E_{m_S,m_I} - E_{m_S-1,m_I} = g_{eff}\mu_B B - 3D_{eff}(^1/_2 - m_S) \quad (2)$$

where

$$g_{eff}{}^2 = \tilde{\mathbf{h}}\cdot\mathbf{g}^2\cdot\mathbf{h} \qquad g_{eff}{}^2 D_{eff} = \tilde{\mathbf{h}}\cdot\mathbf{g}\cdot\mathbf{D}\cdot\mathbf{g}\cdot\mathbf{h}$$

and **h** is the unit vector along magnetic field **B** direction. A fitting of experimental data presented in Figure 3 to eq 2 gave *g*-factors and *D*-splittings as summarized in the Table 1. The best fit is presented by lines in Figure 3, and principal axis directions of the **D**-tensor are marked. The **g**-tensor and **D**-tensor are not collinear, and the D_z direction deviates by about 10° from the Cu−Cu direction in $Cu_2Cl_8^{4-}$ dimer (Figure 1).

The zero-field splitting tensor **D** in binuclear Cu(II) complexes is expected to have contributions from dipole−dipole magnetic interaction and from anisotropic exchange coupling: $\mathbf{D} = \mathbf{D}^{dip} + \mathbf{D}^{ex}$. The maximal fine structure splitting from $\mathbf{D}^{dip}$ is expected along the Cu−Cu direction whereas that from $\mathbf{D}^{ex}$ is expected along the g_z-direction. In our case, the experimentally observed maximal zero-field splitting D_z deviates from the Cu−Cu direction toward the g_z-axis. It means that the both contributions to the **D**-tensor are substantial. The dipolar contribution (in cm^{-1}), in point dipole approximation, can be calculated as

$$D_i^{dip} = 0.325 g_i^2 r^{-3}(1 - 3\cos^2\theta) \quad (3)$$

when the **g**-tensors, of both Cu(II) ions coupled into dimers, are collinear. In $Co(en)_3CuCl_5\cdot H_2O$ the interionic distance is r = 3.722 Å and the $\mathbf{D}^{dip}$ tensor components are

$$D_z^{dip} = -0.0578 \text{ cm}^{-1} \qquad D_y^{dip} = 0.0285 \text{ cm}^{-1} \qquad D_x^{dip} = 0.0260 \text{ cm}^{-1}$$

From D_i^{dip} values and experimental D_i parameters (Table 1) one can calculate $\mathbf{D}^{ex}$ components (assuming negative signs for experimental D_z-values):

$$D_z^{ex} = 0.0378 \text{ cm}^{-1} \qquad D_y^{ex} = -0.0135 \text{ cm}^{-1} \qquad D_x^{ex} = -0.0207 \text{ cm}^{-1}$$

We cannot discuss the D_i^{ex}-values in terms of anisotropic exchange integrals as is usually done[12] since the values were calculated by assuming that the principal axes of the dipole−dipole interaction tensor and the axes of the zero-field splitting are parallel, which is only approximately true (see Figure 1).

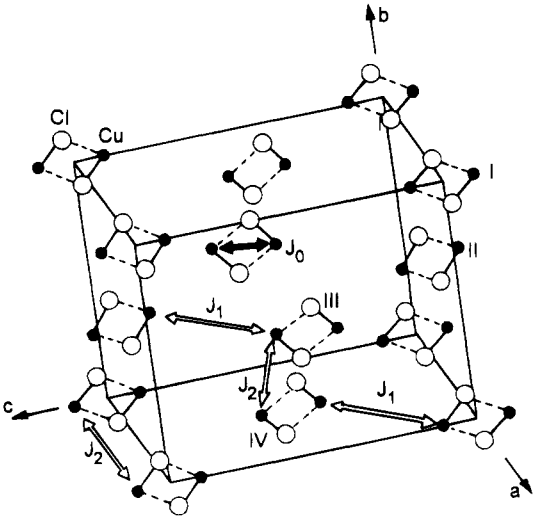

Figure 4. Unit cell of $[Co(en)_3]_2[Cu_2Cl_8]Cl_2\cdot 2H_2O$.[6,9] Only the Cu_2Cl_8 dimers are shown. Interlayer J_1 and intralayer J_2 exchange pathways are shown. J_0 indicates the antiferromagnetic intradimer exchange with singlet−triplet splitting equal to −14.8 cm^{-1}.

Interlayer and Intralayer Exchange Interaction between $[Cu_2Cl_8]^{4-}$ Dimers. The layered structure of $Co(en)_3CuCl_5\cdot H_2O$ suggests that interdimer couplings should be different between dimers in a layer and between dimers located in neighboring layers because of different interdimer distances and different pathways for superexchange transmission. Thus one can assume that superexchange can be described by exchange integral J_1 between layers and J_2 in layers as presented in Figure 4. An observation of the merging effect between EPR lines from inequivalent dimers located in neighboring layers allowed us to determine the value of a weak interdimer coupling J_1 reported in a previous paper.[9] We have found that J_1 decreases linearly on cooling down to 80 K, which was explained in terms of a model with competing ferro- and antiferromagnetic contributions affected by thermal lattice contraction.[13] In this paper we present the J_1 temperature behavior below 80 K (full circles in Figure 5).

The exchange integral between inequivalent sites is derived from an onset of the merging effect between the splitting of EPR lines which are observed in the crystal *bc*-plane for $T >$ 15 K (Figure 2). The method is based on modified Bloch equations, and we have published two forms of the algorithm for fitting of a two-component EPR spectrum with exchange-coupled lines.[6,7] A more compact form of the algorithm is presented below. When two Lorentzian resonance lines with resonance fields B_1 and B_2 and half-width Γ_1 and Γ_2 ($\Gamma = \sqrt{3}/2\Delta B_{pp}$) are exchange coupled with Hamiltonian $H_{ex} = JS_1S_2$, then the resulting EPR spectrum cannot be reproduced as an overlap of two independent lines. The spectrum is broadened, and the central part of the spectrum is averaged when J is not much less than the critical value: $J_{cr} \approx 0.35(B_2 - B_1)$ for narrow lines when $\Gamma/(B_2 - B_1) < 0.05$ or $J_{cr} \approx 0.09(B_2 - B_1)$ when line width Γ is comparable to the line splitting $(B_2 - B_1)$.[14] Such a spectrum with a visible merging effect or a spectrum arising when two lines are fully coalesced can be described by the formulae

(12) Ozarowski, A.; Reinen, D. *Inorg. Chem.* **1986**, *25*, 1704.
(13) Hoffmann, S. K.; Hilczer, W. *Inorg. Chem.* **1991**, *30*, 2210.
(14) Goslar, J.; Hilczer, W.; Hoffmann, S. K.; Krupski, M. *Phys. Stat. Sol. b* **1991**, *167*, 291.

$$Y(B) = N[\{[W_2 - 2(B - B_0)J](W_1^2 + W_2^2) - 4[(B - B_0)W_1 + (\Gamma_0 + J)W_2][(B - B_0)W_2 - (\Gamma_0 + 2J)W_1]\}/(W_1^2 + W_2^2)^2] \quad (4)$$

where

$$W_1 = (B - B_1)(B - B_2) - (\Gamma_1 + K_1)(\Gamma_2 + K_2) + K_1K_2$$

$$W_2 = (B - B_1)(\Gamma_2 + K_2) + (B - B_2)(\Gamma_1 + K_1)$$

and

$$B_0 = (B_1 + B_2)/2 \quad \Gamma_0 = (\Gamma_1 + \Gamma_2)/2 \quad K_1 = JB_1/B_0 \quad K_2 = JB_2/B_0$$

N is a normalization factor proportional to the total number of paramagnetic centers in the sample and describes intensity of a recorded experimental spectrum. All parameters in eq 4 are given in mT, and the relationship between energy and field value of exchange integral J is

$$J[\mathrm{cm}^{-1}] = 0.46686 \times 10^{-3}\, g_0 J[\mathrm{mT}]$$

where g_0 is the g-factor of the central B_0 field. Equation 4 describes the dependence of the amplitude Y of an EPR spectrum recorded in a form of the first derivative of the absorption, as a function of the external magnetic field B swept during the EPR experiment. The equation is valid in the whole range of J-values. For $J = 0$ the equation reduced to a sum of two Lorentzian lines at B_1 and B_2, and for $J > J_{cr}$ the equation describes the shape of the single line formed from two completely merged lines. In the intermediate region eq 4 describes a more complicated shape of the spectrum with two partially resolved lines disturbed by an onset of the merging effect. Using eq 4 one can find the absolute value of J since the merging effect is independent of whether ferro- or antiferromagnetic coupling operates.

Results of a fitting of our experimental data with eq 4 are shown as the full circles in the $J_1(T)$ plot on Figure 5; the open circles for $T > 80$ K are taken from data of the previous paper.[9] The weak exchange J_1 between layers, transmitted via hydrogen bonds and ethylenediamine molecules, strongly decreases on cooling down to about 100 K and then becomes temperature independent with value $J_1 = 0.00325$ cm^{-1}. Below about 18 K our algorithm does not work properly since an additional line splitting appears. Each of two lines split into a doublet with equal line intensity.

Appearance of the splitting is a gradual process and looks like a merging effect. We observed it in detail along crystal c-axis where, because of symmetry reasons, the single resonance line exists at high temperatures. The line width value is maximal at this orientation and where we expect the strongest effect of the splitting. It is shown in Figure 6. A similarity in the temperature behavior of the fine structure doublet to the typical dynamical type merging effect suggested use of the algorithm of eq 4. However the equation is written in the form appropriate for two lines with different g-factors as is clear from differences in K_1, K_2, and J. For the lines of the fine structure doublet, the g-factors are equal and related to the B_0-field. In this case in eq 4, $K_1 = K_2 = J$. We have obtained a perfect fit of eq 4 to experimental spectra in the temperature range 4.2–95 K using a temperature dependent effective J_2 coupling parameter as shown in Figure 6 and plotted by the dashed line in Figure 5.

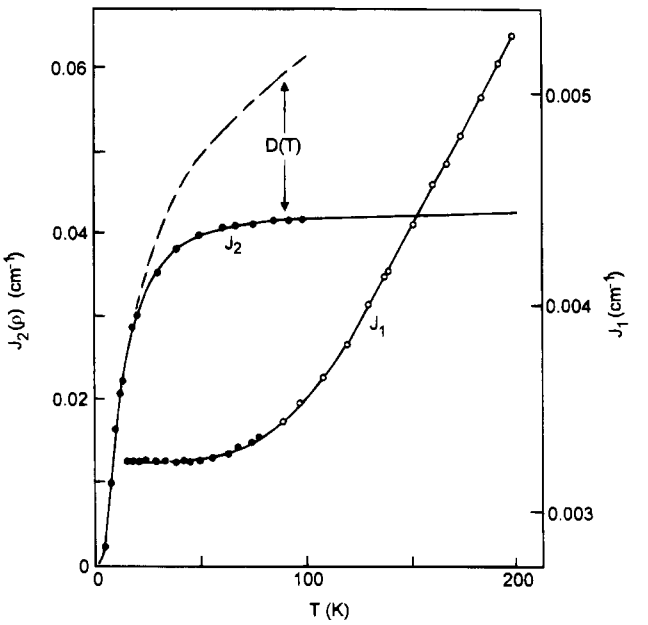

Figure 5. Temperature behavior of interlayer J_1 and intralayer J_2 superexchange coupling between the $[Cu_2Cl_8]^{4-}$ dimers. In the $J_1(T)$ plot the open circles are taken from a previous paper[9] and the solid line is the guide to the eyes. The dashed line describes an effective exchange coupling between dimers located in the same layer obtained from the merging effect assuming a temperature-independent zero-field splitting D. The solid line in the J_2 plot represents thermal triplet density behavior, and the full circles are obtained from experimental data by subtraction of the temperature dependence of the **D**-tensor.

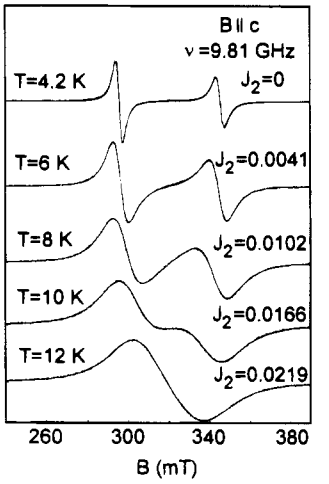

Figure 6. Influence of temperature on the zero-field splitting observed along the crystal c-axis. On the noisy experimental spectra the theoretical lines are superimposed as calculated from eq 4 with a temperature dependent J_2-value. The lines of the doublet are equal in integral intensity at 4.2 K, and the apparent difference in amplitude is due to imperfect alignment of the c-axis along the magnetic field.

The averaging of the fine structure doublet as the temperature is raised can be understood in terms of triplet state density ϱ_T which strongly varies at low temperatures. For antiferromagnetically coupled dimers the ground state is the diamagnetic singlet state possessing paired spins and magnetic properties of the system are related to the excited triplet state which depopulates on cooling. The number of spins in triplet states determines the value of the magnetic susceptibility which can be written as $\chi(T) = \varrho_T\chi_C$, where χ_C is the Curie susceptibility for noninteracting spins and ϱ_T is a triplet state density governed by temperature: $\varrho(T) = [1 + {}^1/_3 \exp(-2J_0/kT)]^{-1}$, where $2J_0$ is singlet–triplet separation.[15] At 4.2 K almost all $[Cu_2Cl_8]^{4-}$ dimers are in the ground diamagnetic singlet state ($S = 0$) and

the magnetic triplet state ($S = 1$) lying 14.8 cm^{-1} higher is nearly depopulated giving the weak EPR spectrum. An average distance between magnetic dimers is then large enough to preclude exchange and/or dipolar coupling between these dimers and fine structure is resolved. Unexpectedly, however, the hyperfine structure is then unresolved and, moreover, the lines are still Lorentzian and continuously narrow with further lowering of temperature. A similar situation appears in EPR spectra of organic free radicals of the TCNQ- and TTF-type charge transfer salts,[15-17] and it is discussed in terms of mobile triplet states, the triplet excitons.[18,19] A rapid triplet exciton motion at low temperatures causes the hyperfine structure to be averaged out to a single Lorentzian line. The exciton mobility mechanism was also introduced to explain a smearing out of the hyperfine splitting in some copper(II) salts.[20,21]

An increase in temperature results in an increase in the thermal population of the excited triplet state. Thus the density of the dimers in magnetic state increases and the average distance between them decreases leading to increase in an effective coupling between the dimers. It is observed as a continuous line broadening followed by a shift toward the center, and at the end lines coalesce into a single line. It appears at the temperature close to that when thermal energy is equal to the singlet−triplet splitting and singlet and triplet states are equally populated. It means that exchange coupling between dimers is stronger than a critical coupling J_{cr}. The effective exchange coupling J_2 affected by triplet density is the coupling between dimers located in the same layer since the interlayer coupling J_1 is too weak at this temperature to produce the merging of the fine structure lines. One can expect that the effective value of J_2 is proportional to the thermal triplet density

$$J_2 \propto \left[1 + {}^1/_3 \exp\left(-\frac{2J_0}{kT}\right)\right]^{-1} \qquad (5)$$

where $2J_0$ is singlet−triplet splitting. A similar type of reduction in interaction was observed in chains of strongly antiferromagnetically coupled Cu(II) ions,[21] in stacked TCNQ molecules[22] and in chromium(III) dimers in the $CsCr_2Cl_9$ crystal.[23]

The proportionality from eq 5 applied to the low-temperature J_2 values from Figure 6 leads to the equation

$$J_2 = 0.05984\left[1 + {}^1/_3 \exp\left(\frac{21.26}{T}\right)\right]^{-1}$$

(with 0.05984 being the best fit parameter) which is plotted as solid line in Figure 5. For $kT > 2J$, when singlet and triplet states are nearly equally populated the J_2-value approaches asymptotically a constant value. At about 100 K, $J_2 = 0.041$ cm^{-1} and it can be assumed as an intralayer exchange coupling between $Cu_2Cl_8^{4-}$ dimers. There exists, however, a distinct discrepancy between $J_2(T)$ dependence (dashed line) determined by thermal triplet density (solid line) and $J_2(T)$ dependence determined from merging effect and described by eq 4. This discrepancy is unnoticeable at low temperatures when the triplet density rapidly falls but becomes pronounced when the two lines are completely coalesced into a single line which continuously narrows on heating. We well know that the algorithm in eq 4 works properly in the whole range of exchange coupling values from the weak exchange limit, through the intermediate region to the fast exchange limit. Thus the observed discrepancy must be due to some other effect.

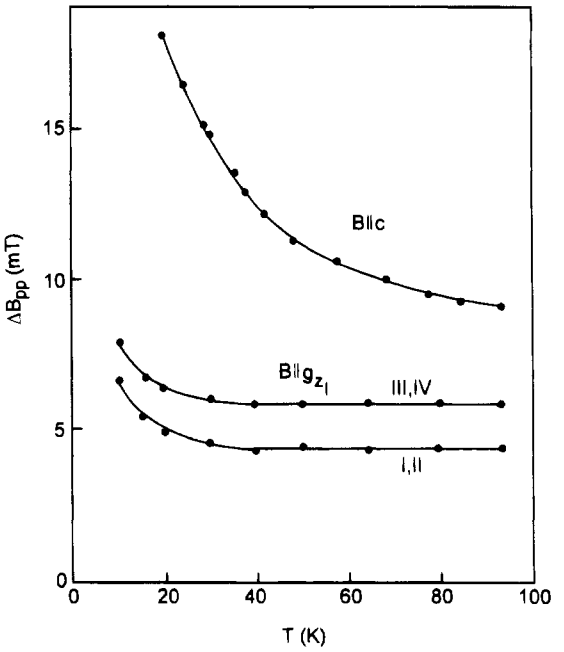

Figure 7. Low-temperature behavior of the line width governed by unresolved zero-field splitting along the c-axis and local g_z-axis of the dimer I.

We postulate that it is due to temperature dependence of the zero-field splitting parameter. It is confirmed by a comparison of the temperature dependence of the line width at different crystal orientations. The dependence along the crystal c-axis and along the principal g_z axis of the dimer I is shown in Figure 7. The c-axis direction lies close to the maximal zero-field splitting whereas along g_z (I) the zero-field splitting is much smaller. It is reflected in ΔB_{pp}-values of the averaged lines. The lines along g_z (I) are much narrower, and moreover a broadening starts only at about 30 K before the critical point whereas along the c-axis the line width is affected by temperature up to 100 K. Assuming that in the temperature range 4.2−100 K two effects contribute to the observed behavior of the EPR spectrum, one can separate the thermal density effect from zero-field splitting D temperature dependence.

Zero-Field Splitting Temperature Dependence. Using J_2-values from eq 5 and B_1 and B_2 as fitting parameters in eq 4 we found that the zero-field splitting $(B_2 - B_1) = 3D_c$ along the c-axis decreases upon heating as is shown by points in Figure 8. Such a type of **D**-tensor behavior is commonly observed for single multielectron ions with $S \geq 1$ as a result of thermal averaging of the crystal field gradient in the ionic site.[24-26] For dimers, such behavior is not expected since the Cu_2Cl_2-bridge geometry is not affected by temperature as is proved by the magnetic susceptibility measurements. Temperature dependence of the susceptibility is well described by the Bleaney−Bowers equation

(15) Chesnut, D. B.; Phillips, W. D. *J. Chem. Phys.* **1961**, *35*, 1002.
(16) Nöthe, D.; Moroni, W.; Keller, H. J.; Soos, Z. G.; Mazumdar, S. *Solid State Commun.* **1978**, *26*, 713.
(17) Hoffmann, S. K.; Corvan, P. J.; Singh, P.; Sethulekshmi, C. N.; Metzger, R. M.; Hatfield, W. E. *J. Am. Chem. Soc.* **1983**, *105*, 4608.
(18) McConnell, H. M. Magnetic Excitations in Molecular Crystals. In *Molecular Biophysics*; Pullman, B., Ed.; Academic Press: New York, 1965; p 311.
(19) Soos, Z. G. *J. Chem. Phys.* **1966**, *44*, 1729.
(20) McGregor, K. T.; Hatfield, W. E. *J. Chem. Phys.* **1975**, *62*, 2911.
(21) McGregor, K. T.; Soos, Z. G. *Inorg. Chem.* **1976**, *15*, 2159.
(22) Graja, A.; Sekretarczyk, G.; Krupski, M. *J. Phys.* **1985**, *46*, 1743.
(23) Beswick, J.; Dugdale, D. E. *J. Phys. C: Solid State Phys.* **1973**, *6*, 3326.
(24) Shrivastava, K. N. *Phys. Rep.* **1975**, *20C*, 139.
(25) Ajiro, Y.; Friedberg, S. A.; Van der Ven, N. S. *Phys. Rev. B* **1977**, *12*, 39.
(26) Rubins, R. S.; Yang, Y. H. *J. Chem. Phys.* **1981**, *75*, 4285.

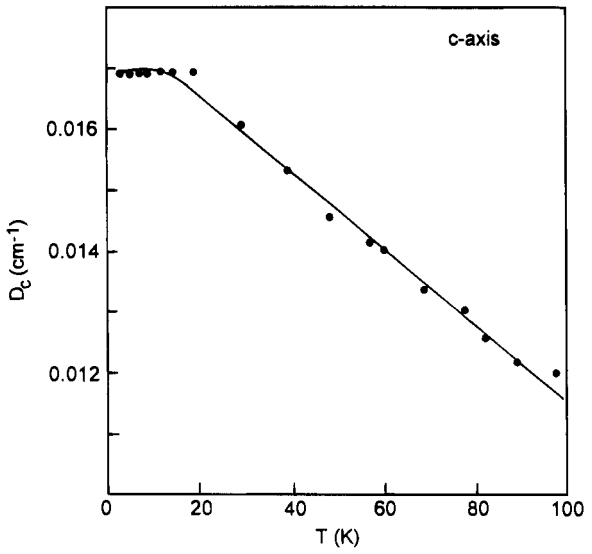

Figure 8. Decrease of zero-field splitting on heating observed along crystal c-axis. The solid line is the best fit to the equation $D(T) = D_0(1 - aT - bT^{-2})$.

$$\chi_m = Ng^2\mu_B{}^2\{3k(T - \Theta)[1 + {}^1/_3 \exp(-2J_0/kT)]\}^{-1}$$

with singlet−triplet splitting $2J_0$ which is temperature independent in the whole temperature range.[9] Since J_0 is very sensitive to even small changes in the dimer bridge geometry as was found for bis(μ-oxo)-[27] and bis(μ-chloro) bridged Cu(II) dimers,[28] one can assume that Cu_2Cl_2-bridge geometry is temperature independent at least within experimental error in J_0, i.e. ± 0.1 cm^{-1}. This error implies that dimer geometry is stable within accuracy of about 3×10^{-3} in Φ/R, where Φ is the Cu−Cl−Cu bridging angle and R is the longer Cu−Cl distance. Thus dipole−dipole coupling contribution to the **D**-tensor can be assumed as temperature independent. Nevertheless, we have observed a decrease of the zero-field splitting on heating in chlorocuprates $[(C_6H_5)_4Sb]_2Cu_2Cl_6$[29] and in $[(C_6H_5)_3(n\text{-Propyl})P]_2Cu_2Cl_6$[30] and a similar behavior was reported for admixtured Cu(II)-Cu(II) pairs in the Zn(N,N-diisopropyldithiocarbamate)$_2$ crystal.[31] We have attributed this to temperature variations of the anisotropic exchange contribution due to a change in thermal population of the vibronic levels of the chlorocuprate complex which are characterized by different anisotropic exchange integrals as discussed in our previous paper.[29] Phenomenologically, our $D(T)$ dependence along c-axis can be described by an equation

$$D(T) = D_0(1 - aT - bT^{-2}) \qquad (6)$$

with parameters $D_0 = 179.11 \times 10^{-4}$ cm^{-1}, $a = 0.0036$, and $b = 0.8470$ that is shown by the solid line in Figure 8. Such equations are commonly used in NQR spectroscopy to describe temperature variations of the nuclear quadrupole resonance frequency.[32,33]

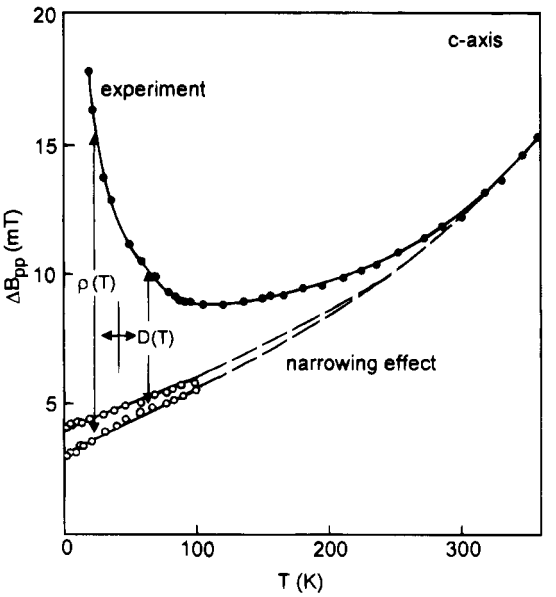

Figure 9. Temperature dependence of the line width along the c-axis. From experimental points (full circles) the triplet density $\varrho(T)$ effect and zero-field splitting $D(T)$ effect were subtracted leading to open circles representing the line width of two "decoupled" fine structure lines. Assuming that at high temperatures the $\varrho(T)$ and $D(T)$ effect are negligible the lines through open circles were extrapolated to fit experimental data for $T > 300$ K. These lines represent a narrowing effect produced by relaxation and/or antisymmetric exchange.

Line Width Temperature Behavior. The line width is angular and temperature dependent with a strange angular dependence in the bc-plane at room temperature (see Figure 2). In all crystal orientations, lines narrow on cooling to about 100 K[9] and then a broadening is observed down to a critical point where the fine structure begins to resolve. We present it for a selected orientation, i.e. along the c-axis, where the line is broadest (Figure 9). During our decoupling procedure, when J_2 was calculated, we found simultaneously the "true" line width values of the two fine structure lines nonperturbed either by the triplet density effect or temperature variations of the **D**-tensor. These calculated values are presented in Figure 9 and show linear temperature behavior, with low-limit values equal to 3.4 and 4.5 mT directly measured from the spectrum at 4.2 K. One can expect that at high temperatures the triplet density effect is negligible, the zero-field splitting is averaged to the single line, and other mechanisms can determine the line width values. Thus we extrapolated "by hand" the decoupled line widths to the experimental point above 300 K (dashed lines in Figure 9). These lines represent a narrowing effect produced by other mechanisms on cooling. Approximately linear temperature dependence of the line width of the "decoupled" lines suggests that it can be due to a spin−phonon modulation of the antisymmetric exchange as was found in many copper(II) compounds.[34-36] However, the relaxation processes of spin−spin type can give a large or even dominant contribution to the line width at low temperatures. Unfortunately, we have not enough data to separate these contributions.

The last two mechanisms determine the line width at high temperatures. When temperature decreases, a contribution from unresolved fine structure, described as $D(T)$ in Figure 9,

(27) Hatfield, W. E. In *Theory and Applications of Molecular Paramagnetism*; Boudreaux, E. A., Mulay, L. N., Eds.; Willey: New York, 1976; Chapter 7.
(28) Hoffmann, S. K.; Towle, D. K.; Hatfield, W. E.; Chaudhuri, P.; Wieghardt, K. *Inorg. Chem.* **1985**, *24*, 1307.
(29) Gatteschi, D.; Goslar, J.; Hilczer, W.; Hoffmann, S. K.; Zanchini, C. *Inorg. Chem.* **1989**, *28*, 3395.
(30) Gatteschi, D.; Goslar, J.; Hilczer, W.; Hoffmann, S. K.; Zanchini, C. *Mol. Phys. Rep.* **1994**, *5*, 174.
(31) Sreehari, N.; Manoharan, P. T. *Mol. Phys.* **1988**, *63*, 1077.
(32) Kushida, T.; Benedek, G. B.; Bloembergen, N. *Phys. Rev.* **1956**, *104*, 1364.
(33) Maćkowiak, M.; Stankowski, J.; Zeks, B.; Blinc, R. *Phys. Rev. B* **1979**, *19*, 1651.
(34) Seehra, M. S.; Castner, T. G. *Phys. Kondens. Mater.* **1968**, *7*, 185.
(35) Willett, R. D.; Extine, M. *Chem. Phys. Lett.* **1973**, *23*, 281.
(36) Geiser, U.; Gaura, R. M.; Willett, R. D.; West, D. X. *Inorg. Chem.* **1986**, *25*, 4203.

increases and becomes dominated by the triplet density effect at low temperatures. Thus $Co(en)_3CuCl_5 \cdot H_2O$ crystals present a rare case where the unresolved zero-field splitting is a dominant contribution to the line width at intermediate temperatures. This contribution allows us to explain the line width angular dependence in the *bc*-plane at room temperature (Figure 2). The maximal line width value appears along the direction where maximal *D*-splitting was found at 4.2 K (Figure 3). Thus, even at room temperature the zero-field contribution to the ΔB_{pp} is observable. At 4.2 K when fine structure lines are well resolved, the angular ΔB_{pp} variations follow the *g*-factor behavior with the maximal ΔB_{pp} value along the g_z-direction. It indicates that ΔB_{pp} is governed by an unresolved hyperfine splitting which is expected to be maximal along the local *z*-axis of the crystal field for a $d_{x^2-y^2}$ ground state and much less in perpendicular directions.

Acknowledgment. This research was supported by the Committee of Scientific Research under Grant No. KBN-2-0979-91-01.

Registry Number (supplied by author): 28852-88-2.

IC940305C